Journal of Applied Electrochemistry **30**: 1209–1222, 2000.

A SERS spectroelectrochemical investigation of the interaction of 2-mercaptobenzothiazole with copper, silver and gold surfaces

R. WOODS, G.A. HOPE and K. WATLING
School of Science, Griffith University, Nathan, Queensland 4111, Australia

Received 4 January 2000; accepted in revised form 20 June 2000

Key words: chemisorption, copper, electrodes, gold, 2-mercaptobenzothiazole, Raman spectroscopy, silver, X-ray photoelectron spectroscopy

Abstract

The interaction of the sulfide mineral flotation collector, 2-mercaptobenzothiazole, with silver, copper and gold surfaces has been investigated by surface enhanced Raman scattering (SERS) spectroscopy. 2-mercaptobenzothiazole, the copper, silver and gold compounds of this species, and the dithiolate, 2,2′-dithiobis(benzothiazole) were characterised by ^{13}C NMR and Raman spectroscopy to provide a basis for identifying surface species. SERS investigations showed that, at pH 4.6 where the solution species is in the protonated form, and at 9.2, where it is present as the ion, adsorption on each metal occurs over a wide potential range. Attachment of the organic compound occurs through bonding between the exocyclic sulfur atom and metal atoms in the surface. X-ray photoelectron spectroscopy confirmed that the adsorbed layer was of monolayer thickness. Adsorption of the protonated 2-mercaptobenzothiazole occurs on copper at pH 4.6 at potentials below that at which charge transfer adsorption commences.

1. Introduction

2-Mercaptobenzothiazole has been applied for many years as a flotation collector in the form of its soluble sodium salt. This compound is marketed by Cytec Industries as Aero promoter 400 and is present in mixtures with dithiophosphates in its Aero 400 series. These collectors are recommended for the treatment of sulfide ores, precious metal ores, gold-bearing pyrite, and tarnished and secondary copper, lead and zinc minerals. 2-Mercaptobenzothiazole and derivatives of this molecule have recently been examined [1] as part of a program to develop selective flotation collectors based on known chelating properties. 2-Mercaptobenzothiazole has also been recognized [2] as an effective corrosion inhibitor for copper and its alloys.

2-Mercaptobenzothiazole has a pK_a of 6.93 at 20 °C [3] and hence is present in acid media as the unionized protonated form (HMBT) which could adopt either the thione or the thiol structure:

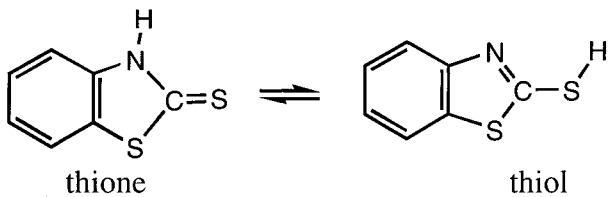

thione thiol

u.v.–vis. spectroscopic studies [2, 4] have shown that HMBT is present in acidic aqueous solutions predominantly as the thione. However, recent Raman and infrared spectroscopic studies [5] were interpreted in terms of the HMBT occurring in solution in the thiol form.

In basic media, 2-mercaptobenzothiazole exists as the thiol ion (MBT^-):

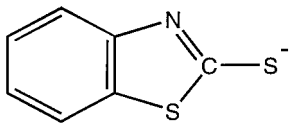

Similarly to a range of other thiols, 2-mercaptobenzothiazole can be oxidized to the dithiolate, 2,2′-dithiobis(benzothiazole) $(MBT)_2$ [6]:

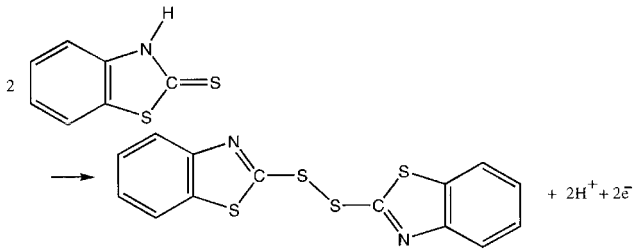

The interaction of 2-mercaptobenzothiazole with galena (PbS) has recently been investigated by Szargan et al. [7] using synchrotron radiation-excited photoelectron spectroscopy (SR-XPS), a technique which provides a strongly enhanced surface sensitivity compared to conventional XPS. The mineral was examined after

immersion in aqueous solutions in equilibrium with air over a range of collector concentrations and solution pH values. The S 2p spectra obtained after treatment of galena with the collector were interpreted in terms of two different adsorbate species. A chemisorbed monolayer was first formed in which MBT is bonded to lead atoms in the mineral and is oriented perpendicular to the surface. Charge transfer chemisorption was followed by the formation of a layer of collector oxidation products that could include $(MBT)_2$. With preoxidized galena surfaces, $Pb(MBT)_2$ was precipitated onto the mineral surface. The presence of $Pb(MBT)_2$ was indicated also by an additional component in the Pb 4f spectra. The identification of the initial layer as chemisorbed was substantiated by the observation that there was no shift in the Pb 4f binding energy when only this species was present. The absence of core electron energy shifts on chemisorption has been reported for the interaction of other collectors on metal and sulfide surfaces [8]. It was proposed [8] that this property could be utilized to distinguish chemisorption from phase formation.

FTIR investigations [9] of the adsorption of 2-mercaptobenzothiazole and two of its derivatives on galena showed that the collector becomes bonded to metal atoms in the mineral surface through the exocyclic sulfur atom. A similar conclusion was reached [4] from infrared spectroscopic studies of the adsorption of this organic species on pyrite (FeS_2), coupled with extended Hückel molecular orbital calculations.

Infrared reflection and X-ray photoelectron spectroscopic studies of the interaction of 2-mercaptobenzothiazole with copper in relation to metal corrosion were interpreted [2] in terms of the formation of a thin polymeric film of CuMBT on the surface. This film was considered to act as a barrier against corrosive environments. In that work, the surface of the copper was not reduced to remove oxides prior to exposure to 2-mercaptobenzothiazole and hence the multilayer could have been formed by reaction of the organic species with surface oxides.

Surface-enhanced Raman scattering (SERS) and X-ray photoelectron spectroscopies were applied [5] to characterize adsorbed layers of 2-mercaptobenzothiazole on silver and on gold. The authors assumed that a self-assembled monolayer on each metal was generated by exposure to a 10^{-3} mol dm^{-3} solution of the organic species in ethanol. They concluded that 2-mercaptobenzothiazole adsorbs in its thione form on silver with its molecular plane flat on the surface and in the thiol form on gold with the molecule sited perpendicular. They did not appear to consider the possibility of charge transfer adsorption involving deprotonation to form a metal–MBT bond.

SERS spectroscopy has been applied to investigate the mode of adsorption of thiourea [10, 11] and *O*-isopropyl-*N*-ethylthionocarbamate [12] on copper and of ethyl xanthate on copper [13, 14], silver [13–15] and gold [13, 16]. In these studies, the bulk metal compounds were characterized by ^{13}C NMR as well as by Raman spectroscopy. The present communication presents analogous studies of the interaction of 2-mercaptobenzothiazole with copper, silver and gold surfaces.

2. Experimental details

2.1. *Preparation of mercaptobenzothiazole compounds*

2-Mercaptobenzothiazole was supplied by Cytec Industries, Inc., as Aero 400 promoter which is the sodium salt in aqueous alkali. This solution was acidified to precipitate the acid form, 2-mercaptobenzothiazole (HMBT). The dithiolate, 2,2′-dithiobis(benzothiazole) ($(MBT)_2$), was prepared by oxidising the aqueous alkaline solution with a solution of potassium persulfate and the precipitate recovered by filtration. Silver(I) 2-mercaptobenzothiazole (AgMBT) was precipitated from a solution of 2-mercaptobenzothiazole in ethanol by the addition of aqueous silver nitrate [17]. The precipitated compound was washed with water and with ethanol. Copper(I) 2-mercaptobenzothiazole (CuMBT) was prepared by adding CuCl dissolved in an aqueous KCl solution to 2-mercaptobenzothiazole in ethanol [18]. The precipitate was washed as for the silver compound. Gold(I) 2-mercaptobenzothiazole (AuMBT) was prepared by adding aqueous gold chloride to HMBT in ethanol. The precipitate was treated as for the other metal compounds.

Khullar and Agarwala [17] reported that copper(II) bis(2-mercaptobenzothiazole) ($Cu(II)(MBT)_2$) was formed when ethanolic solutions of $CuCl_2$ and 2-mercaptobenzothiazole were combined. The Raman spectrum obtained when this procedure was followed, however, showed that the precipitate was a mixture of CuMBT and $(MBT)_2$. This result is in agreement with the conclusion reached by Ohsawa and Suëtaka [2]. Thus, the interaction of copper ions with 2-mercaptobenzothiazole is similar to that with xanthate. In each case oxidation of the collector to the dithiolate occurs at a lower potential than that of the copper(I) compound to the copper(II).

2.2. *Voltammetry and rest potential measurements*

Voltammograms were recorded for copper, silver, gold and platinum electrodes in deoxygenated buffer solutions of pH 4.6 and 9.2 using an ADInstruments MacLab/4e interfaced with a Macintosh computer. A potential program was applied that consisted of switching the potential from the open circuit value to the lower potential limit, holding at this value for 2 s, and then applying a triangular potential scan. Voltammetry was carried out with the electrode in the buffer solution alone and after 2-mercaptobenzothiazole had been added to make the solution 10^{-3} mol dm^{-3} or 10^{-2} mol dm^{-3} in this compound for the pH 4.6 and 9.2 solutions, respectively. Potentials were referred to a Ag–AgCl–KCl (saturated) reference electrode and converted to the standard hydrogen electrode (SHE)

scale taking the potential of the reference to be 0.20 V on this scale. All potentials in this paper are presented on the SHE scale.

Open circuit potentials were measured for copper, silver, gold and platinum electrodes in solutions of 2-mercaptobenzothiazole dissolved in 0.1 mol dm^{-3} Na_2SO_4 with the pH adjusted with NaOH and H_2SO_4. Potentials were determined against a saturated calomel electrode (SCE) with a Keithley 2000 multimeter that had an input impedance of 10^{12} Ω and were converted to the SHE scale taking the value of the SCE to be 0.245 V on this scale.

2.3. ^{13}C Nuclear magnetic resonance

High resolution ^{13}C NMR spectra of MBT^- dissolved in aqueous alkaline solution, HMBT in acetone-d_6, and $(MBT)_2$ in chloroform-d, were recorded using a Varian Unity 400 spectrometer operating at 100 MHz. The field induced decay was recorded in 32k data points, spectral width of 22 kHz, 24 μs (90°) pulse, and a cycle time of 30 s.

2.4. *X-ray photoelectron spectroscopy*

X-ray photoelectron spectra were recorded with a Kratos XSAM 800 electron spectrometer using AlK_α X-rays, a take-off angle of 90°, and an analyser pass energy of 20 eV. The spectrometer was operated using the Dayta Surface Analysis Software System 98.1 of the Interface Analysis Centre of Bristol University, U.K. Silver electrodes were held at a selected potential in a 10^{-4} mol dm^{-3} solution of MBT^- in borate buffer of pH 9.2, immersed in deoxygenated, deionized water for 1 min, excess water removed, and then inserted into the spectrometer. The Ag 3d, S 2p, and N 1s spectra were recorded and analyzed using Dayta software. Spectra were also recorded for AgMBT placed on conducting copper tape.

2.5. *Raman spectroscopy*

Raman spectra for HMBT, $(MBT)_2$, aqueous MBT^-, and the model compounds, benzene, 1:2 dimethyl benzene, thiazole and thiophene were obtained with a Renishaw Raman spectrograph (multichannel compact Raman analyser) that has a rotary encoded grating stage, and an internal two stage Peltier cooled (−70 °C) CCD detector. The spectral resolution was 5 cm^{-1}, and the wavenumber reproducibility 0.1 cm^{-1}. The incident radiation was conveyed from a Spectra Physics Argon ion laser of 514.5 nm excitation, through a fibre optic Raman probe.

The compounds CuMBT, AgMBT and AuMBT decomposed under the laser at full power (20 mW) and Raman spectra were recorded with the spectrometer in the standby mode (2 mW). SERS spectra with a silver electrode were also recorded with the Renishaw spectrometer.

SERS spectra for copper and gold electrodes employed a Perkin Elmer System 2000 NIR FT-Raman spectrometer, equipped with a Spectron Laser system SL 301 Nd:YAG laser emitting at 1064 nm, a quartz beam splitter, and an InGaAs detector operated at room temperature. Spectra were recorded at room temperature with a total of 50 scans at a resolution of 4 cm^{-1} and a laser power of 200 mW.

The electrochemical cell used in the SERS investigations with the FT-Raman instrument was as described previously [10]. It was constructed of borosilicate glass with a flat window at one end. The working electrode was mounted on an assembly constructed from PTFE and was positioned close to the window. It follows the design devised by Fleischmann et al. [19]. Copper and gold electrodes of 6 mm diameter were prepared from metal of 99.99% purity. With copper, the surface was electrochemically roughened prior to obtaining SERS spectra by oxidation–reduction cycling (ORC) in 2 mol dm^{-3} H_2SO_4 [20]. This procedure involved the application of 4–5 cycles between −0.3 and 0.7 V with a polarisation period of approximately 30 s before reversing the polarity. With gold, ORC was carried out between 0.1 and 0.9 V in 1 mol dm^{-3} KCl acidified with HCl.

In the cell employed with the Renishaw spectrometer, the working electrode was a silver flag attached to a silver wire. The electrode was heated in a furnace at 450 °C for 16 h and then roughened by applying ORC in 1 mol dm^{-3} KCl acidified with HCl between −0.2 and 0.6 V after initially reducing at −0.5 V.

SERS spectra were recorded for 10^{-4} mol dm^{-3} 2-mercaptobenzothiazole in solutions of pH 4.6 and 9.2 that were deoxygenated with 'high purity' nitrogen. In the acid medium, the collector will be present as HMBT and in the base as MBT^-. The buffer solution of pH 4.6 was 0.05 mol dm^{-3} sodium acetate, 0.05 mol dm^{-3} acetic acid, and that of 9.2 was 0.05 mol dm^{-3} sodium tetraborate. In each case, the working electrode was held at a potential just above the hydrogen evolution potential in the buffer solution alone to remove surface oxides and then the 2-mercaptobenzothiazole added.

Most SERS spectra were recorded *in situ* under potential control. Some spectra were recorded on immersed electrodes. For these measurements, spectra were recorded after the solution had been drained from the cell. The removal of solution was carried out under a constant flow of nitrogen to avoid ingress of oxygen from the atmosphere during emersion and the recording of spectra.

SERS spectra were also recorded for 2-mercaptobenzothiazole adsorbed onto a silver sol. The colloid was prepared by adding 10 cm^3 of 1% w/v trisodium citrate dropwise to 500 cm^3 of 10^{-3} mol dm^{-3} silver nitrate solution maintained at the boiling point, and refluxing for 1 h [21].

3. Results and discussion

3.1. *Voltammetry and rest potentials*

Voltammograms for copper, silver, gold and platinum electrodes in an acetate buffer of pH 4.6 containing 0

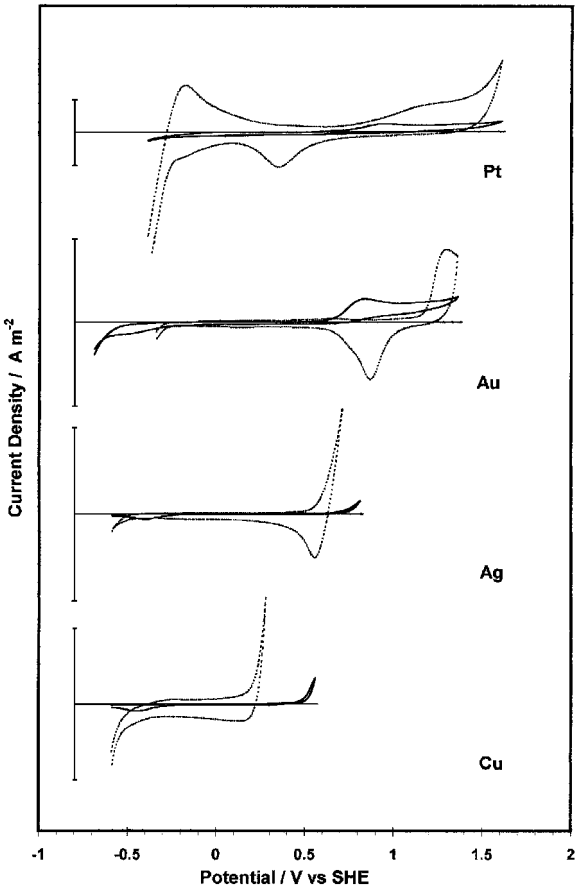

Fig. 1. Voltammograms for copper, silver, gold and platinum electrodes in solution of pH 4.6 containing (----) 0, and (——) 10^{-3} mol dm^{-3} 2-mercaptobenzothiazole. Ordinate bar interval corresponds to a current density of 5 A m^{-2} centred on zero.

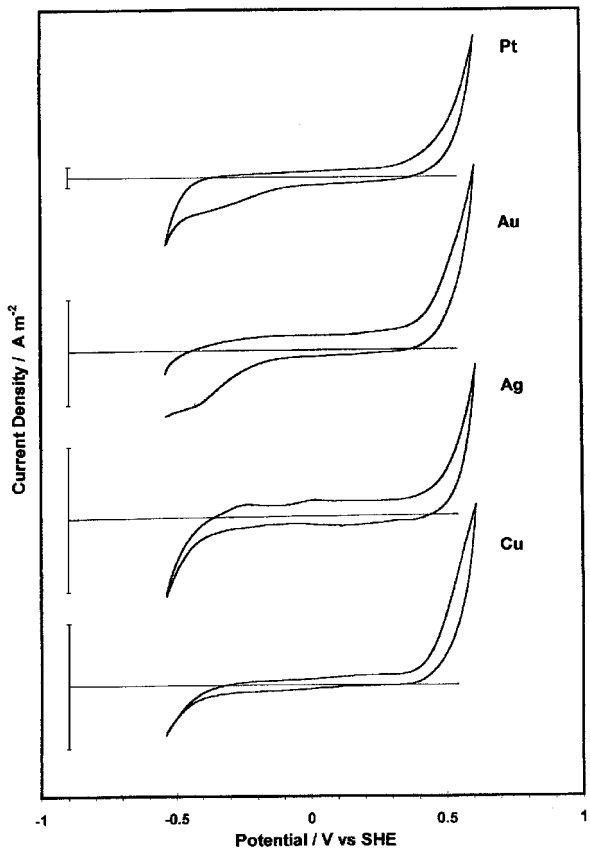

Fig. 2. Voltammograms for copper, silver, gold and platinum electrodes in solution of pH 9.2 containing 10^{-2} mol dm^{-3} 2-mercaptobenzothiazole. Ordinate bar interval corresponds to a current density of 0.25 A m^{-2} centred on zero.

and 10^{-3} mol dm^{-3} HMBT are presented in Figure 1. For each metal, the lower potential limit of the scan corresponds to the onset of hydrogen evolution. In the absence of the collector, copper and silver exhibit anodic currents due to dissolution of the metal. Platinum and gold display currents in the positive potential region due to the adsorption and desorption of oxygen derived from water [22]. With platinum, significant currents are also observed at negative potentials and these arise from the adsorption and desorption of hydrogen and from the hydrogen evolution reaction [22]. The major change observed when HMBT is present is the inhibition of all of these processes. This indicates that the organic species is adsorbed on each of the electrodes surfaces throughout the potential range examined. Extension of the negative potential limit did not alter the CV shape significantly.

With gold, an anodic wave is observed in the presence of HMBT commencing at about 0.6 V (Figure 1). There is a corresponding cathodic wave commencing at about −0.2 V. Similar features are seen in the voltammogram for platinum, replacing the hydrogen and oxygen adsorption phenomena observed in the absence of HMBT. These features can be confidently assigned to the oxidation of HMBT to $(MBT)_2$:

$$2\,HMBT \rightarrow (MBT)_2 + 2\,H^+ + 2\,e^- \quad (1)$$

Voltammograms for electrodes of the four metals in borate buffer of pH 9.2 containing 10^{-2} mol dm^{-3} MBT^- are presented in Figure 2. In each case, an anodic current is observed at potentials above about 0.4 V. Corresponding cathodic currents can be seen below about −0.2 V. As in the acid solution, it is concluded that the process responsible for the anodic current is oxidation to $(MBT)_2$. At pH 9.2 the reaction is

$$2\,MBT^- \rightarrow (MBT)_2 + 2\,e^- \quad (2)$$

Alternative reactions, such as oxidation of the metal MBT compound to the disulfide, for example,

$$CuMBT + H_2O \rightarrow (MBT)_2 + CuO + 2\,H^+ + 2\,e^- \quad (3)$$

would appear to be ruled out since the potential at which such reactions take place is expected to be different for each metal.

As pointed out above, the features on the voltammograms are indicative of adsorption of 2-mercaptobenzothiazole throughout the potential range studied. There are no obvious features that can be assigned to charge

transfer adsorption to form a chemisorbed monolayer, namely, in acid media:

$$HMBT \rightarrow (MBT)_{ads} + H^+ + e^- \quad (4)$$

or in base:

$$MBT^- \rightarrow (MBT)_{ads} + e^- \quad (5)$$

In addition, there are no features that can be ascribed to the development of a metal MBT compound. It is possible that charge transfer oxidative adsorption of 2-mercaptobenzothiazole commences at potentials below the lower limit of the voltammometric scan and that this process could occur in the absence of dissolved oxygen by coupling with the cathodic evolution of hydrogen. In this way, the electrode surface would be coated with MBT_{ads} and/or the metal MBT compound before the scans were initiated. Alternative explanations are that the adsorption is not discernible on voltammograms because the rate of adsorption is slow, and because the adsorption density corresponding to a monolayer of such a large molecule as 2-mercaptobenzothiazole is quite small, that is, monolayer coverage requires a significantly smaller charge for this compound than it does for collectors such as a xanthate. The characteristics of 2-mercaptobenzothiazole adsorption would thus result in an inability to distinguish the current due to adsorption from background charging currents. It was noted by Yoon and Basilio [23] in investigations on copper/thionocarbamate systems that voltammetry may not provide unequivocal information on the adsorption of large collector molecules. In order to determine collector adsorption as a function of potential in such situations, it is necessary to apply spectroelectrochemical techniques.

To determine if adsorption occurs at underpotentials, as has been demonstrated for xanthate [22], dithiophosphate [22], and thionocarbamate [12] collectors, it is necessary to know the value of the reversible potential for the formation of the metal compound. At attempt was made to determine the reversible values from the rest potentials displayed by each of the metals in solutions containing different concentrations of 2-mercaptobenzothiazole. However, no quantitative information could be obtained from rest potential measurements regarding the metal–metal MBT couples.

Rest potentials were found to be irreproducible with the recorded values drifting over time even when a voltmeter with very high impedance ($10^{12}\ \Omega$) was employed. Under apparently identical conditions, the measured potentials varied by as much as ± 30 mV. Also, the values did not accurately follow the concentration dependence expected for a Nernstian relationship. With a conventional multimeter that had an input impedance of $10^6\ \Omega$, the electrodes became polarized, as evidenced by a slow decrease in the magnitude of the measured potential after the voltmeter was switched into the circuit, and recovery to the initial value when the circuit was opened again. These observations are consistent with studies on the effect of the addition of 2-mercaptobenzothiazole on the impedance of platinum electrodes immersed in copper electroless plating baths [24]. It was found that the presence of low concentrations of 2-mercaptobenzothiazole resulted in the formation of a capacitive electrode/solution interface with a polarization resistance in the MΩ range.

Rest potentials were recorded after holding the potential of the electrode in the hydrogen evolution region as well as for freshly abraded electrode surfaces. The measured potentials for the former situation slowly increased with time to give values in the same range as observed for the latter. Comparison of these values with the voltammograms in Figures 1 and 2 indicates that they do not correspond to the formation of a metal MBT phase, but to oxidation to $(MBT)_2$. For each metal, this will occur on an adsorbed layer of MBT which, as pointed out above, is highly resistive and hence renders accurate determination of the rest potential difficult. The most stable and reproducible rest potential was that observed for a gold electrode in 0.1 mol dm^{-3} 2-mercaptobenzothiazole in alkaline media. The measured value of −0.040 V corresponds to a formal potential for Reaction 2 of −0.10 V.

Within the limits set by the irreproducibility of the measurements, the rest potential was found to be independent of pH in basic solution as expected for Reaction 2. When the solution was acidified, the rest potential increased, with the dependence on pH being consistent with Reaction 1. From the formal potential derived for Reaction 2, and the pK_a of 6.93 for 2-mercaptobenzothiazole, the formal potential of Reaction 1 will be 0.31 V.

Goold and Finkelstein [25] reported that the standard reduction potential for sodium mercaptobenzothiazole was −0.049 V. This value presumably refers to alkaline solution and hence to Reaction 2. It is similar to that reported in the present work, considering the difficulty in making precise measurements. Note that the value reported by Goold and Finkelstein was incorrectly cited as 0.049 V by Finkelstein and Poling [6].

3.2. *Characterization of bulk species by ^{13}C NMR*

Chemical shifts for the various carbon atoms in HMBT, MBT^- and $(MBT)_2$ are presented in Table 1. Carbon atoms 1–6 correspond to the benzene ring with C5 being attached to the nitrogen and C6 to the sulfur in the heterocyclic ring. C7 is the carbon atom in the heterocyclic ring attached to the nitrogen and to both sulfurs.

It can be seen that the chemical shifts for C1–C6 in MBT^- and $(MBT)_2$ are similar. The greater value of the shift for C7 most likely arises from the negative charge on the exocyclic sulfur atom. The chemical shifts for C1, C5, C6 and C7 are significantly different from those of HMBT. This is explained by HMBT adopting the thione structure (see Section 1.). In the other two molecules,

Table 1. ^{13}C NMR chemical shifts for 2-mercaptobenzothiazole compounds

C atom	MBT^- in aq. soln.	HMBT in $(CD_3)_2O$	$(MBT)_2$ in CD_3Cl
1	118	112	121
2	120	121	123
3	122	124	125
4	125	127	127
5	136	130	136
6	153	141	154
7	181	191	168

there is a double bond between the nitrogen and C7 which coordinates with the benzene ring to distribute electron density.

There is no evidence for the presence of a second conformational isomer for HMBT and hence the thiol form of this compound is not present to any significant extent.

3.3. *Raman spectra of bulk species*

Raman spectra for solid HMBT and $(MBT)_2$, and for a concentrated aqueous alkaline solution of MBT^-, are shown in Figure 3. The characteristic bands are presented in Table 2. The assignment of Raman bands was made on the basis of previous reports of vibrational spectra of 2-mercaptobenzothiazole in the literature,

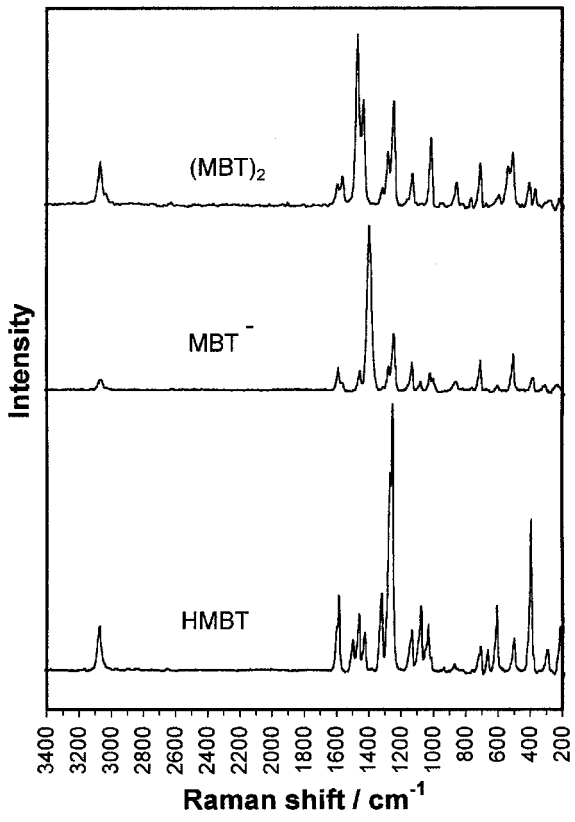

Fig. 3. Raman spectra of HMBT, MBT^- and $(MBT)_2$.

Table 2. Characteristic Raman bands for 2-mercaptobenzothiazole compounds

HMBT	MBT^-	$(MBT)_2$	Assignment
3161 vw			NH stretch
3071 m	3066 m	3067 m	CH stretch
	3029 w	3033 w	CH stretch
1597 sh	1589 m	1594 w	Bz ring stretch
1583 m	1562 s	1561 m	NCS stretch
1495 m			N—C═S stretch (thioamide I)
1458 m	1455 m	1468 s	Bz ring stretch
1423 m	1398 vs	1432 s	NCS ring stretch
1318 m		1315 vw	NH bend (thioamide II)
1268 s	1276 m	1279 m	CH in-plane bend
1252 vs	1246 s	1242 s	NCS ring stretch
1130 m	1131 m	1126 m	CH in-plane bend
1074 m	1078 w		Bz ring or SCS antisymmetric stretch
1048 m			C═S stretch (thioamide III)
1029 m	1021 m		CH deformation
1011 m	1002 w	1010 s	CH bend
868 w	865 m	853 w	CH out-of-plane bend
706 m	708 m	705 m	C—S stretch
662 m			NH deformation
606 m	604 w	591 vw	CS stretch
		536 m	SS stretch
499 m	505 m	503 m	Bz ring deformation
393 s	385 w	403 w	Bz ring deformation
213 m	226 vw	218 vw	Bz ring deformation

and of Raman spectra recorded for compounds containing the same basic elemental groups. These compounds were benzene, 1:2 dimethyl benzene, thiazole, and thiophene.

The Raman spectrum from HMBT contains bands due to NH vibrations, and to NH—C═S combination vibrations, also known as the thioamide I, II, and III bands. The assignment of these bands is supported by their absence in the spectra for MBT^- and $(MBT)_2$, and confirms that the solid HMBT exists in the thione form. This identification is consistent with the ^{13}C NMR results (Section 3.2) and the conclusion reached by Oshawa and Suëtaka [2]. It is also in agreement with computer calculations based on AM1 (Austin Model 1), a widely used semi-empirical force field theory, indicated [26] that the heat of formation of the thione to be about 10% less than that of the thiol isomer. It is in disagreement with the conclusion reached by Sandhyarani et al. [5] that the thiol form was present in solution. These authors based their assignment on the appearance of a weak band at 2461 cm^{-1} that they attributed to the S—H stretch of the thiol form. The S—H stretching vibration of thiols gives a strong band in Raman spectra [27], whereas the band that Sandhyarani et al. assigned to this vibration was very weak. Since the ^{13}C NMR spectrum for HMBT in acetone displays only one chemical shift for each of the carbon atoms in the molecule, the presence of both conformational isomers in aqueous media is unlikely. Furthermore, the band at 2461 cm^{-1} can be assigned to a vibration mode of the benzene ring of HMBT, since weak bands are observed in the Raman spectrum of benzene at 2460, 2550 and 2621 cm^{-1}. In the present work, a very weak band was

discerned at 2629 cm^{-1} in Raman spectra from HMBT and this also can be assigned to the benzene ring.

The band near 3170 cm^{-1}, that arises from the N—H symmetric stretch in the solid state, is much stronger in infrared than in Raman spectra [27]. To further substantiate the proposed structure of HMBT, FTIR spectra were also run on this compound. The spectrum observed was the same as reported by Oshawa and Suëtaka [2]; the presence of a band at 3113 cm^{-1} confirmed that HMBT in the solid phase exists in the thione form.

The spectrum of $(MBT)_2$ displays a band at 536 nm that can be assigned to the S—S bond. This assignment is substantiated by the absence of such a band in the spectra of the other species.

Raman spectra for the copper, silver and gold MBT compounds are presented in the Figures and Tables listing SERS spectra. As expected, the bands assigned to vibrations of the benzene ring do not vary significantly for the three compounds. There is a difference in the metal–sulfur stretch vibration, the wavenumber decreasing in the order Cu > Ag > Au as expected for the coinage metals. There is a corresponding increase in the band for the NCS ring stretch near 1400 cm^{-1}. This could reflect a decrease in the degree of interaction between the N-atom and neighbouring metal MBT molecules that will diminish the double-bond character of the NS bond.

3.4. *SERS spectra*

3.4.1. *Silver*

SERS spectra were recorded for a silver electrode at controlled potentials in a 10^{-4} mol dm^{-3} MBT^{-}, 0.05 mol dm^{-3} sodium tetraborate solution (pH 9.2). They were essentially the same when the potential was in the range $\geqslant -0.7$ V $\leqslant 0.1$ V and when recorded *in situ* or on an emersed electrode. SERS spectra for −0.5 V are presented in Figure 4 and the characteristic bands for −0.7 and −0.5 V are listed in Table 3. The band at about 3370 cm^{-1} is characteristic of water [28, 29] and arises from scattering by solvent molecules. In subsequent figures presented here, this peak has been eliminated in the background correction.

It can be seen from Table 3 that the SERS spectra exhibit bands for each of the basic elemental groups. This demonstrates that 2-mercaptobenzothiazole retains its molecular integrity when adsorbed on the silver surface. The similarity between the SERS spectra and the Raman spectrum for AgMBT also indicates that the organic species is bonded to the surface through the exocyclic sulfur atom. Most bands in the SERS spectra occur at identical wavenumbers, within experimental error, to those for AgMBT. An exception is that for the NCS vibration at about 1400 cm^{-1}, which is shifted to lower wavelengths by about 10 cm^{-1}. This indicates that

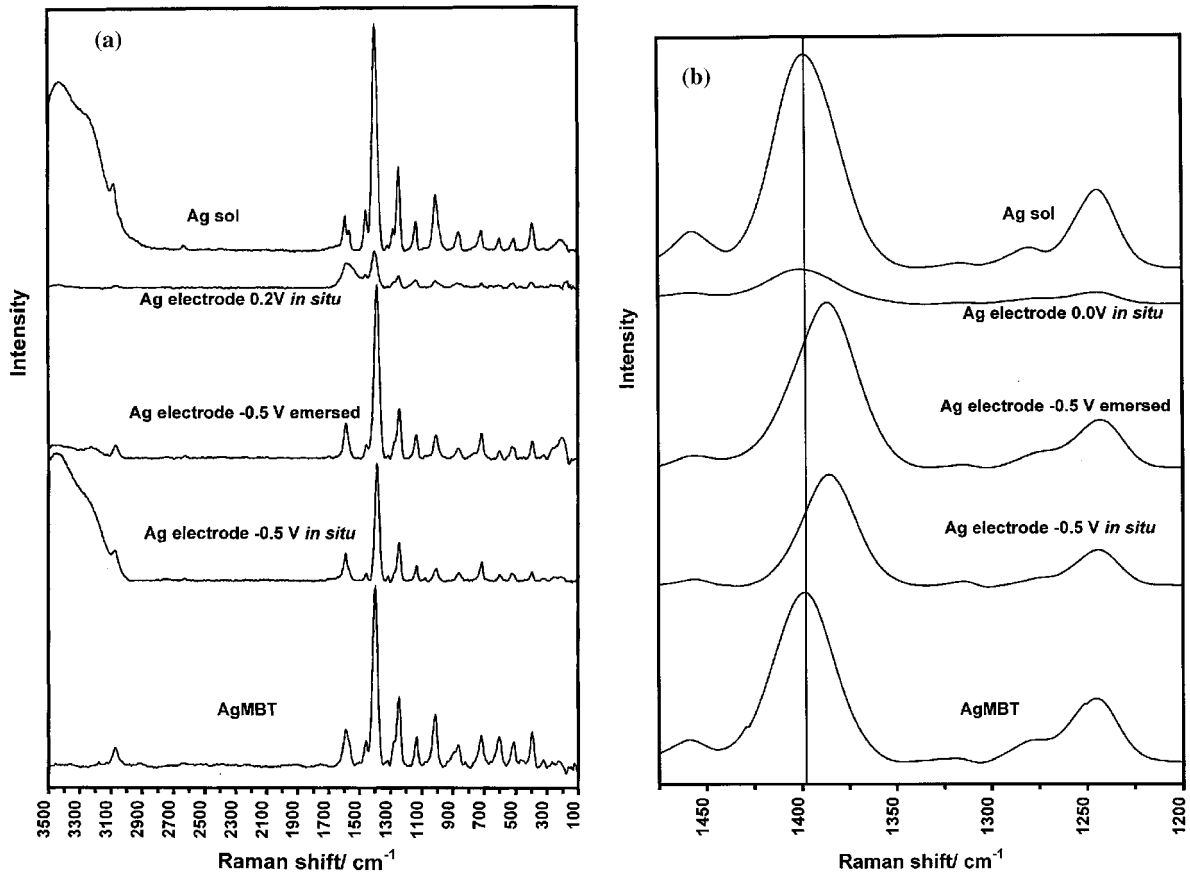

Fig. 4. SERS spectra for 10^{-4} mol dm^{-3} 2-mercaptobenzothiazole on a silver electrode at pH 9.2 and on a silver colloid of pH 8.2 compared with the Raman spectrum of AgMBT. (a) Wide range; (b) selected region, vertical line is position of major band for AgMBT.

Table 3. SERS spectra for silver electrode in 10^{-4} M MBT^-

AgMBT	Ag; pH 9.2; −0.7 V; *in situ*	Ag; pH 9.2; −0.5 V; *in situ*	Ag; pH 9.2; −0.5 V; immersed	Ag, pH 9.2; +0.2 V; *in situ*	Ag sol	Assignment
3072 m	3074 m	3073 m	3072 m	3072 m	3082 m	CH stretch
1589 m	1570 m	1591 m	1590 m	1587 m	1593 m	Bz ring stretch
1566 m	1567 sh	~1560 sh			1565 m	NCS ring stretch
1459 m	1458 m	1457 m	1459 m	1459 m	1459 m	Bz ring stretch
1399 vs	1386 vs	1387 vs	1388 vs	1402 vs	1400 vs	NCS ring stretch
1319 w	1317 w	1316 w	1318 vw		1318 vw	Thioamide II
1280 w	1280 w	1278 w	1277 m		1282 m	CH in-plane bend
1247 s	1246 m	1246 s	1244 s	1247 m	1246 s	NCS ring stretch
1135 m	1132 m	1133 m	1134 m	1133 m	1136 m	CH in-plane bend
1013 s	1008 m	1010 m	1010 m	1009 m	1010 m	CH bend
868 m	864 m	862 m	864 w		864 m	CH out-of-plane bend
721 m	714 m	714 m	714 m	715 m	718 m	CS stretch
604 m	601 m	601 m	602 w		600 m	CS stretch
517 m	523 m	521 m	520 w		510 w	Bz ring deformation
393 m	394 m	395 m	395 m		394 w	Bz ring deformation
320 w	314 w	314 w	319 w		315 vw	MS stretch

the surface species differs slightly from that of the bulk compound as was found by Szargan et al. [7] for adsorption of 2-mercaptobenzothiazole on galena. It is not possible to ascertain from the SERS spectra if MBT is adsorbed at underpotentials since the reversible potential for the formation of AgMBT is not known.

Hydrogen is evolved at the silver surface at potentials < -0.7 V and hence spectra were not recorded in this region. It is apparent that the MBT surface layer on silver electrodes does not develop into a substantial multilayer at potentials $\leqslant 0.1$ V since the SERS spectrum, which is derived from the initial layer bonded to the electrode surface, was not affected by an increase in potential within this range. Polarization at 0.2 V did, however, result in a significant change; the spectrum at this potential is included in Figure 4 and the characteristic bands listed in Table 3. The intensity of each of the bands was lower than that obtained at lower potentials and there was a higher background. This is indicative of a multilayer of AgMBT being formed with the resulting spectrum being derived from the bulk phase. It can be seen that the bands observed for the surface held at 0.2 V, including that for the NCS stretch, was the same as that for AgMBT. The electrode current density at this potential falls rapidly with time as an insulating multilayer grows over the electrode surface.

SERS spectra were also recorded for a silver sol in a 2-mercaptobenzothiazole solution of the same composition as for the silver electrode. The pH of the colloid was 8.2. The resulting spectra are also presented in Figure 4 and Table 3, and all the band positions in this case are identical, within experimental error, to those for solid AgMBT. The difference between the SERS spectra for the electrode and sol systems is considered to result from the different manner of formation of the surface species. Silver ions will be specifically adsorbed at the surface of the silver sol and, indeed, it is the presence of these species that stabilizes the colloid. When 2-mercaptobenzothiazole is added, the silver ions will react to deposit AgMBT in the same form as in the bulk compound. This compound formation neutralizes the surface charge on the colloid and results in the precipitation of the colloid particles.

Metal MBT compounds are considered [17] to consist of linear chains in which the metal atom is bonded to the sulfur in one molecule and the nitrogen in another. When 2-mercaptobenzothiazole interacts with a silver electrode surface, the organic species will become bonded to silver atoms and, since the silver atoms are fixed in the surface, additional bonding to nitrogen atoms in the adsorbed MBT will be restricted. Thus, the double bond character of the nitrogen carbon bond will be retained and the NCS vibration expected to occur at a lower wavenumber. This is a possible explanation of the shift in the frequency of the NCS band between adsorbed MBT and AgMBT. It is noted that the position of the NCS band in $(MBT)_2$ is greater than that of the metal MBT compounds even though the NC bond in this compound will retain the double bond character. It is possible that the difference could be due to the charge distribution being different for the metal compounds and the disulfide.

SERS spectra for a silver electrode in a 10^{-4} mol dm^{-3} HMBT, 0.05 mol dm^{-3} acetic acid, 0.05 mol dm^{-3} sodium acetate (pH 4.6) are presented in Figure 5 and the characteristic bands listed in Table 4. As at pH 9.2, the SERS bands occur at the same frequencies as AgMBT, except for the NCS vibration near 1400 cm^{-1}. Again the NCS band is shifted about 10 cm^{-1} to lower values. At this pH, no upper potential was observed at which AgMBT was formed in sufficient quantity to obscure the spectrum from the initial layer.

No spectra indicative of $(MBT)_2$ were observed on silver electrodes. It should be noted that the potential region explored with SERS spectroscopy was below that at which a current increase due to oxidation to $(MBT)_2$ was observed on the voltammograms shown in Figures 1 and 2.

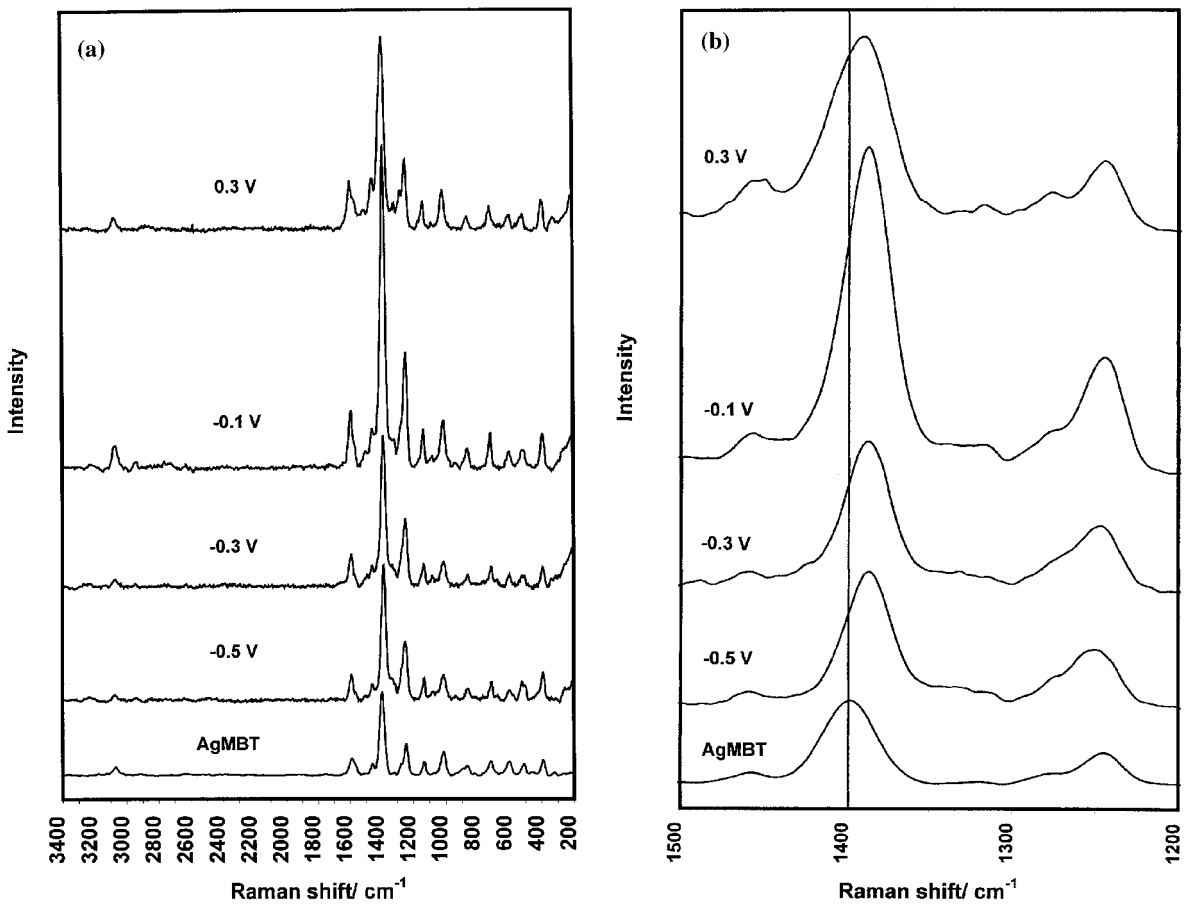

Fig. 5. SERS spectra for silver electrode in 10^{-4} mol dm^{-3} 2-mercaptobenzothiazole at pH 4.6 compared with Raman spectrum of AgMBT. Background corrected. (a) Wide range; (b) selected region: vertical line is position of major band for AgMBT.

Table 4. SERS spectra of silver electrode in 10^{-4} M HMBT at pH 4.6

AgMBT	−0.5 V	−0.3 V	−0.1 V	0.3 V	Assignment
3072 m	3083 w	3076 w	3069 m	3079 m	CH stretch
1589 m	1591 m	1591 m	1591 m	1593 m	Bz ring stretch
1566 m	1564 sh	1566 sh	1567 sh	1565 sh	NCS ring stretch
1459 m	1461 m	1461 m	1459 m	1455 m	Bz ring stretch
1399 vs	1388 vs	1387 vs	1388 vs	1391 vs	NCS ring stretch
1319 w	1316 vw	1317 vw	1315 vw	1317 w	Thioamide II
1280 w	1275 w	1276 w	1289 m	1278 m	CH in-plane bend
1247 s	1251 s	1248 s	1246 s	1245 m	NCS ring stretch
1135 m	1134 m	1135 m	1135 m	1135 m	CH in-plane bend
1013 s	1015 m	1015 m	1012 m	1014 m	CH bend
868 m	864 m	862 m	864 m	861 m	CH out-of-plane bend
721 m	715 m	715 m	716 m	721 m	CS stretch
604 m	603 m	601 m	601 m	600 m	CS stretch
517 m	516 m	514 m	513 m	515 m	Bz ring deformation
393 m	393 m	394 m	392 m	393 m	Bz ring deformation
320 w	312 vw			321 vw	MS stretch

3.4.2. *Copper*

SERS spectra for a copper electrode at controlled potentials in a 10^{-4} mol dm^{-3} MBT^-, 0.05 mol dm^{-3} sodium tetraborate solution (pH 9.2) are presented in Figure 6 and the characteristic bands listed in Table 5. It can be seen that most of the bands occur at the same frequency as for CuMBT but, as with silver, the NCS vibration near 1400 cm^{-1} is shifted to lower values. Thus, again, the initial monolayer differs from the bulk compound and the explanation for this difference is expected to be the same.

The characteristics of the analogous spectra recorded in the acetate buffer of pH 4.6 can be seen from Figure 7 and Table 6. For potentials $\geqslant -0.1$ V, the SERS spectra were similar to that for CuMBT with the NCS band again occurring at a lower wavenumber. Thus, an adsorbed layer of MBT occurs in this potential range similar to that on silver in both solutions and on copper at pH 9.2.

The SERS spectrum at −0.5 V differs from those at potentials $\geqslant -0.1$ V. It can be seen from Figure 7 and Table 6 that the spectrum is now similar to that for HMBT. Also, the spectrum at −0.3 V displays bands similar to those at higher potentials as well as to HMBT. It is suggested that the initial adsorbate is HMBT and, since all bands arising from this molecule are displayed, adsorption will not involve charge transfer. It is possible that adsorption involves π-bonding between the surface and the aromatic ring of the HMBT molecule. Such adsorption is known to occur with a range of aromatic compounds [30].

As the potential is increased, it is apparent that oxidative charge transfer between the electrode and the adsorbate occurs with the removal of the hydrogen atom

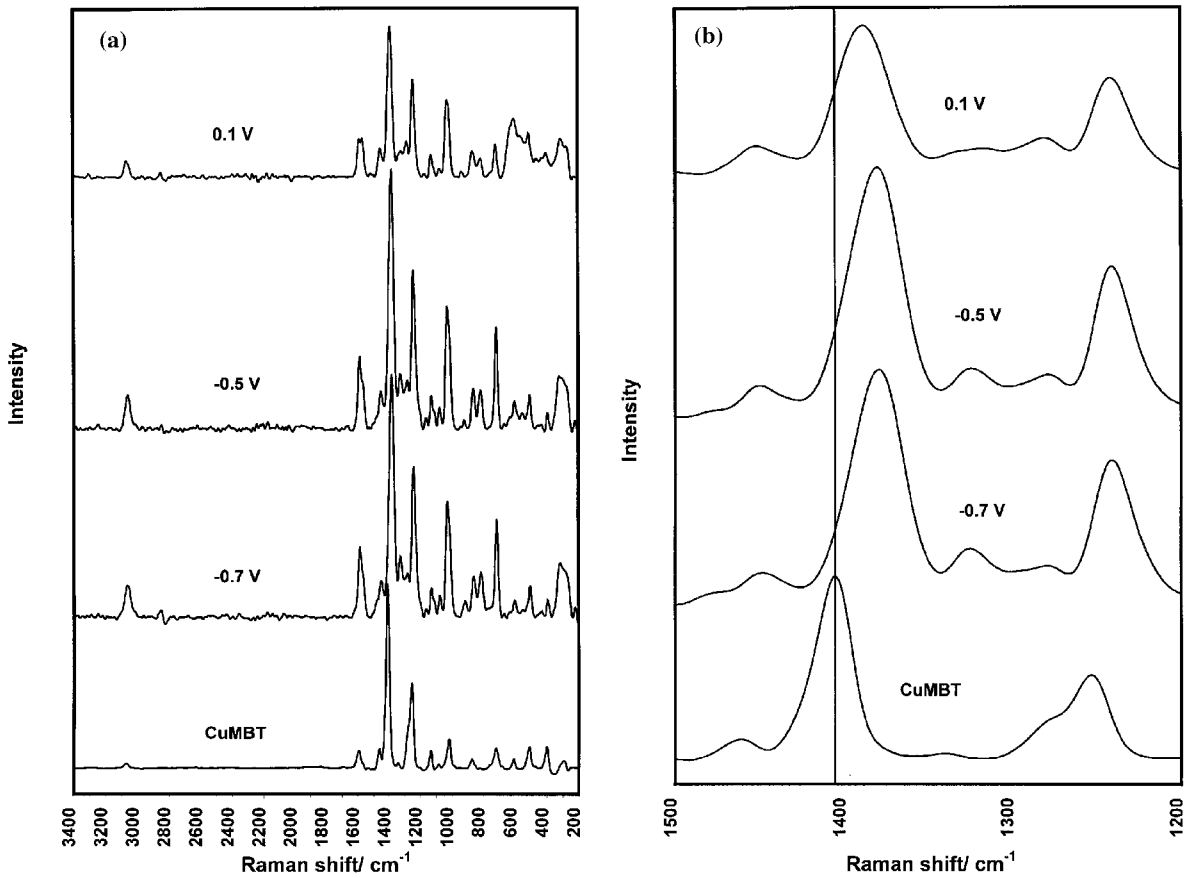

Fig. 6. SERS spectra for copper electrode in 10^{-4} mol dm^{-3} 2-mercaptobenzothiazole at pH 9.2 compared with Raman spectrum of CuMBT. Background corrected. (a) Wide range; (b) selected region: vertical line is position of major band for CuMBT.

Table 5. SERS spectra for copper electrode in 10^{-4} M MBT^- at pH 9.2

CuMBT	−0.7 V	−0.5 V	0.1 V	Assignment
3072 w	3060 w	3063 w	3068 w	CH stretch
1589 m	1584 m	1585 m	1586 m	Bz ring stretch
1564 w	1563 m	1563 m	1564 m	NCS ring stretch
1462 m	1451 m	1453 m	1454 m	Bz ring stretch
1405 vs	1379 s	1383 s	1389 s	NCS ring stretch
1340 vw	1327 m	1327 w	1333 w	Thioamide II
1277 m	1277 m	1279 m	1279 m	CH in-plane bend
1251 s	1242 s	1241 s	1242 s	NCS ring stretch
1133 m	1129 m	1130 m	1129 m	CH in-plane bend
1082 w	1076 w	1079 w		Bz ring or SCS anti-symmetric stretch
	1028 m	1027 m	1029 m	CH deformation
1015 m	1013 m	1013 m	1014 m	CH bend
873 w	861 m	864 m	867 m	CH out-of-plane bend
	812 m	812 m	813 m	
720 m	716 m	717 m	718 m	CS stretch
608 w	602 w	601 w	604 w	CS stretch
509 m	504 w	505 m	506 w	Bz ring deformation
400 m	395 m	395 w	399 w	Bz ring deformation
296 w				MS stretch

from the nitrogen to form a hydrogen ion in solution. The attachment to the surface is then by bonding between surface copper atoms and the exocyclic sulfur atom of 2-mercaptobenzothiazole.

3.4.3. *Gold*

SERS spectra for a gold electrode at different controlled potentials in 10^{-4} mol dm^{-3} 2-mercaptobenzothiazole at pH 9.2 and 4.6 are presented in Figures 8 and 9, respectively. The characteristic bands are listed in Table 7. The spectra in both acid and alkaline media did not vary significantly with change in potential and, as with copper in both solutions and with silver in acid media, the formation of thick multilayers of the metal compound that would attenuate the SERS signal did not occur.

It can be seen from Figures 8 and 9 and Table 7 that, in general, the SERS spectra display bands analogous to those of AuMBT. As with silver and copper, the major peak that is assigned to a NCS ring stretch vibration is shifted to lower wavenumbers compared to the metal compound. This indicates that, again, the initial layer differs from the bulk species. In contrast to the SERS spectra displayed by other metals, however, the major peak includes a shoulder on the high wavenumber side. This indicates that two different adsorbed species are present on the gold surface. It is possible that a multilayer is present throughout the potential range studied and that part of the initial chemisorbed layer becomes bonded through the nitrogen to an MBT radical in the overlaying AuMBT. An alternative explanation is that there are two types of adsorption

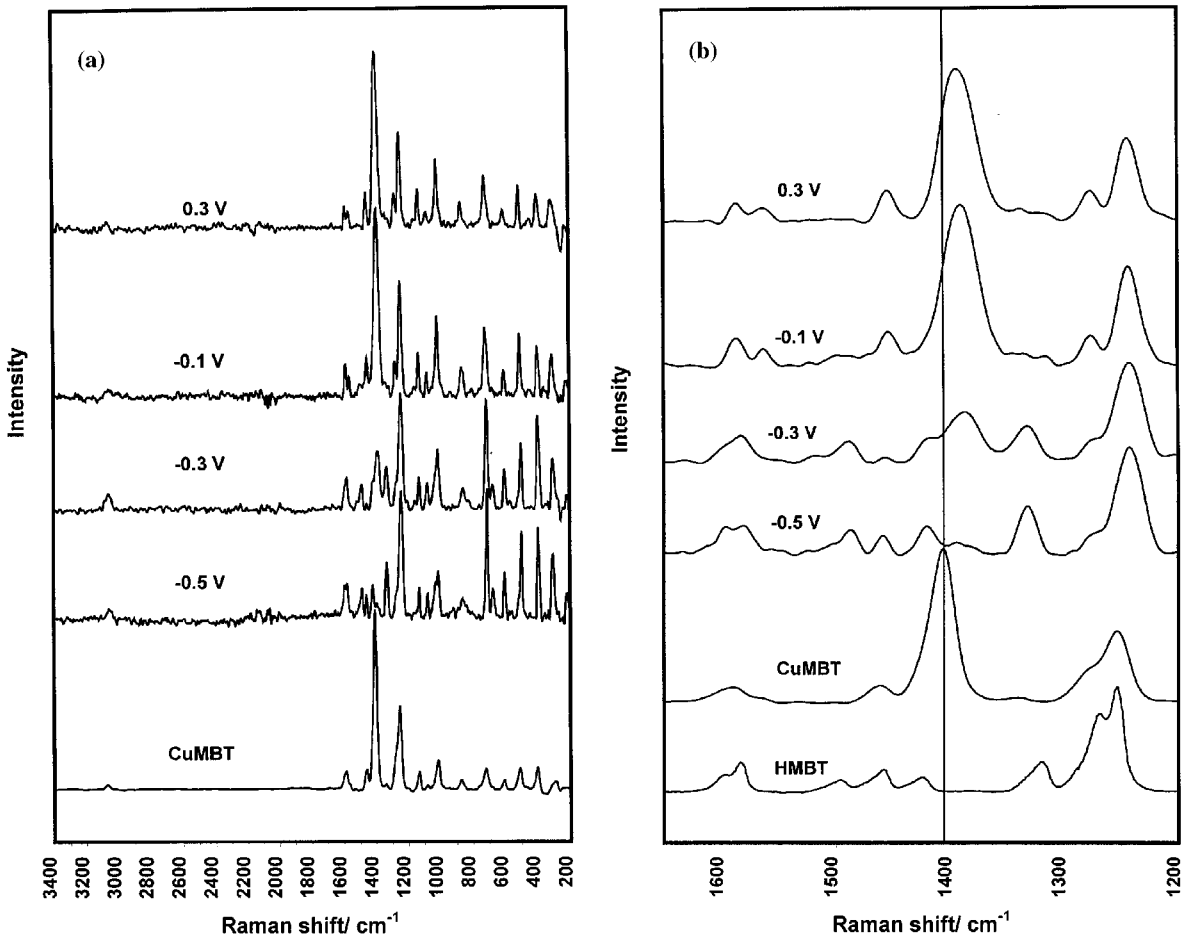

Fig. 7. SERS spectra for copper electrode in 10^{-4} mol dm^{-3} 2-mercaptobenzothiazole at pH 4.6 compared with Raman spectrum of CuMBT. Background corrected. (a) Wide range; (b) selected region including spectrum for HMBT: vertical line is position of major band for CuMBT.

Table 6. SERS spectra for copper electrode in 10^{-4} M HMBT at pH 4.6

CuMBT	HMBT	−0.5 V	−0.3 V	−0.1 V	0.1 V	Assignment
	3161 vw					NH stretch
3072 w	3071 m	3059 w	3063 w	3060 w	3066 m	CH stretch
	1597 sh	1597 m	1596 sh			Bz ring stretch
1589 m	1583 m	1580 m	1583 m	1587 m	1588 m	Bz ring stretch
1564 w				1563 w	1565 m	NCS ring stretch
	1495 m	1487 m	1488 m			Thioamide I
1462 m	1458 m	1458 m	1457 m	1454 m	1454 m	Bz ring stretch
1405 vs	1423 m	1420 m	1421 m	1390 vs	1393 vs	NCS ring stretch
		1394 w	1387 m			
1340 vw						
	1318 m	1331 m	1332 m			Thioamide II
1277 m	1268 s		1274 sh	1276 m	1276 m	CH in-plane bend
1251 s	1252 vs	1242 s	1242 s	1243 s	1245 s	NCS ring stretch
1133 m	1130 m	1130 m	1131 m	1130 m	1129 m	CH in-plane bend
1082 w	1074 m	1079 m	1080 m	1080 m	1077 w	Bz ring or SCS anti-symmetric stretch
	1048 m					Thioamide III
	1029 m	1027 m	1031 sh	1030 sh		CH deformation
1015 m	1011 m	1012 m	1012 m	1013 m	1013 s	CH bend
873 w	868 w	865 w	858 w	860 m	867 m	CH out-of-plane bend
720 m	706 m	708 s	710 s	717 s	718 m	CS stretch
	662 m	674 m	676 m			NH wag
608 w	606 m	603 m	603 m	603 m	604 m	CS stretch
509 m	499 m	497 m	498 m	505 m	506 m	Bz ring deformation
400 m	393 s	394 s	394 s	395 m	396 m	Bz ring deformation
296 w	292 w					MS stretch

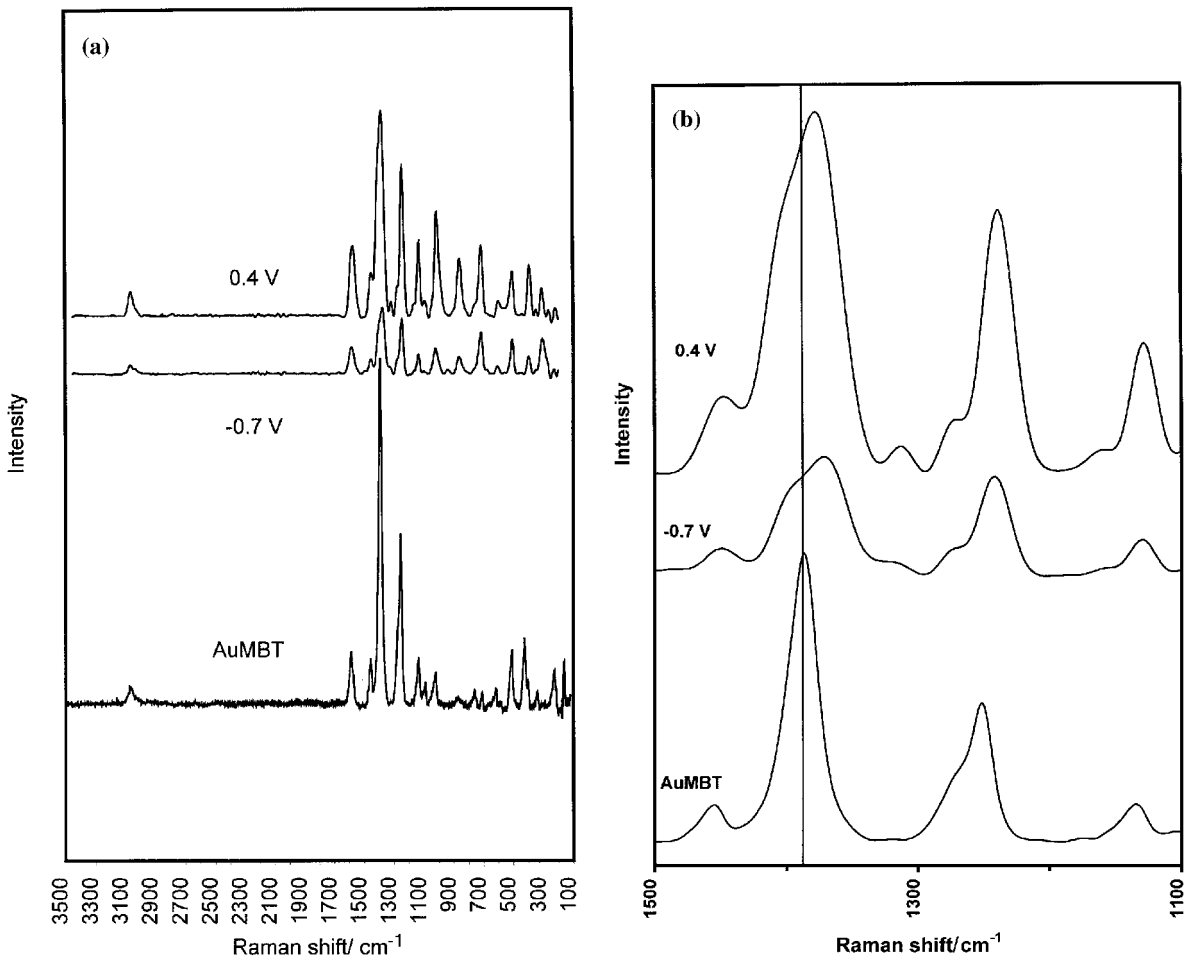

Fig. 8. SERS spectra for gold electrode in 10^{-4} mol dm^{-3} 2-mercaptobenzothiazole at pH 9.2 compared with Raman spectrum of AuMBT. Background corrected. (a) Wide range; (b) selected region: vertical line is position of major band for AuMBT.

site on the gold surface with correspondingly two different MBT orientations. Electrochemical and XPS investigations [31] of alkanethiolate monolayers on evaporated gold films have provided evidence for the existence of two different adsorption binding sites on the surface of this metal.

3.5. *X-ray photoelectron spectroscopy*

The Raman spectra indicate that the 2-mercaptobenzothiazole film on the surface of the three metals under most conditions is very thin, that is, the order of a monolayer, since the SERS effect is observed. To confirm this conclusion, XPS studies were carried out on a silver electrode held for 2 min at −0.4 V, and one for 5 min at 0.0 V, in 10^{-4} mol dm^{-3} MBT^- at pH 9.2. AgMBT was also investigated as a reference material for quantitative analysis.

The relative integral counts of the Ag 3d, S 2p, and N 1s spectra of AgMBT were 1:0.12:0.048. The corresponding relative integral counts for the silver electrodes, recorded under the same instrumental conditions, were 7.15:0.053:0.050 and 6.15:0.052:0.048 for the electrodes held at −0.4 and 0.0 V, respectively. Taking the integral ratios for AgMBT to correspond to the atomic ratios for Ag:S:N of 1:2:1, the integrals for the electrodes correspond to respective ratios of 16:1:2 and 14:1:2. The sulfur integrals are more reliable than the nitrogen since the N 1s spectrum is on the side of a silver energy loss line which has a high intensity for the electrodes. Thus, it is concluded that the Ag:MBT ratios for the spectra from the electrodes held at −0.4 and 0.0 V are 16:1 and 14:1, respectively. Thus, most of the Ag 3d signal is derived from the bulk silver metal and this is indicative of the surface layer being restricted to that of a chemisorbed MBT monolayer.

4. Conclusions

SERS spectroscopy shows that oxidative charge transfer adsorption of 2-mercaptobenzothiazole occurs on copper, silver and gold surfaces with attachment to the surface involving bonding between the exocyclic sulfur atom in the organic compound and metal atoms in the surface. The major band assigned to a NCS stretch vibration is shifted to lower wavenumbers for the initial layer on all three metals and this is indicative of this layer being MBT chemisorbed on metal sites in the

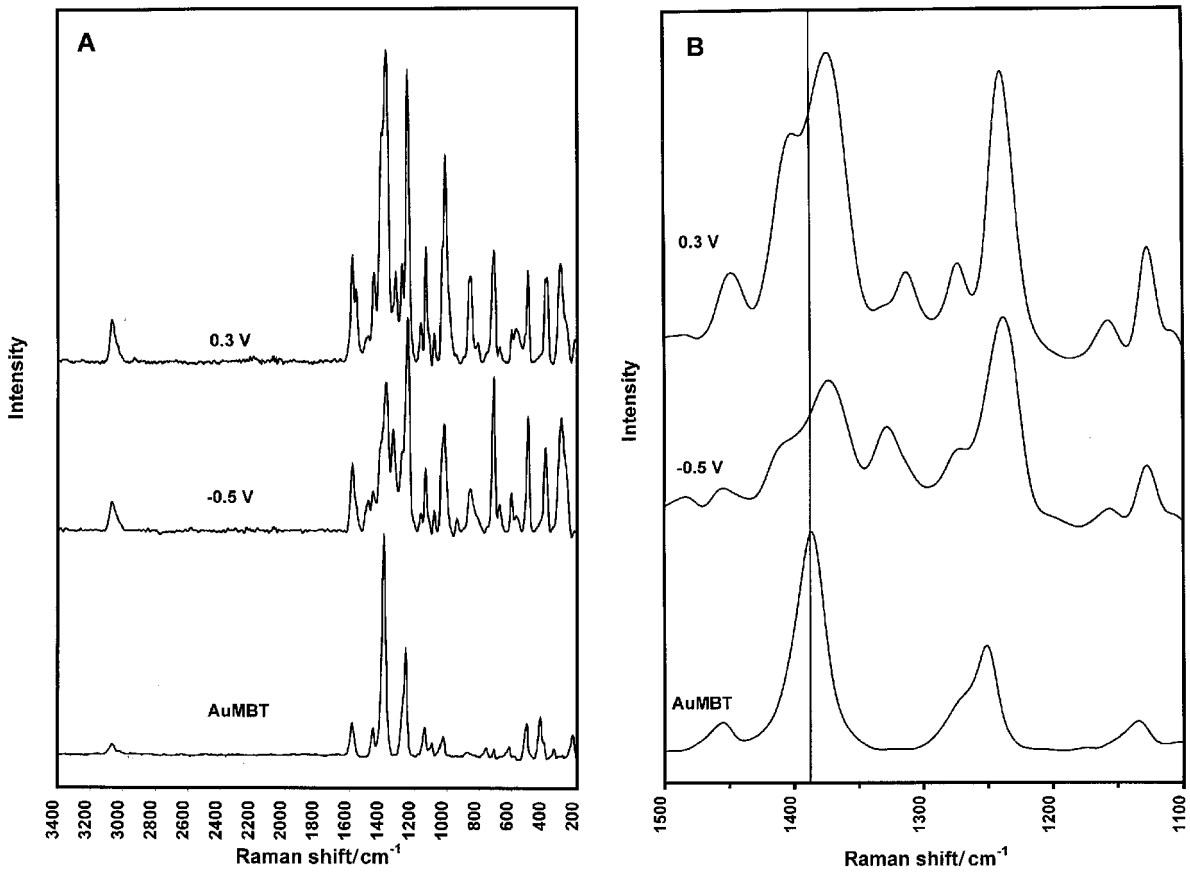

Fig. 9. SERS spectra for gold electrode in 10^{-4} mol dm^{-3} 2-mercaptobenzothiazole at pH 4.6 compared with Raman spectrum of AuMBT. Background corrected. (a) Wide range; (b) selected region: vertical line is position of major band for AuMBT.

Table 7. SERS spectra of gold electrode in 10^{-4} M 2-mercaptobenzothiazole

AuMBT	−0.7 V; pH 9.2	0.4 V; pH 9.2	−0.5 V; pH 4.6	0.3 V; pH 4.6	Assignment
3067 w	3065 w	3065 w	3067 w	3067 w	CH stretch
1587 m	1581 m		1582 m	1583 m	Bz ring stretch
1573 m	1566 m	1566 m	1561 m	1561 m	NCS stretch
1457 m	1450 m	1449 m	1456 m	1449 m	Bz ring stretch
1389 vs	1394 sh	1400 sh	1410 sh	1403 sh	NCS ring stretch
	1371 s	1376 s	1374 s	1374 s	NCS ring stretch
1315 w	1311 w	1313 w	1328 m	1313 m	Thioamide II
1273 sh	1274 sh	1273 sh	1274 sh	1273 sh	CH in-plane bend
1252 s	1242 s	1239 s	1238 s	1240 s	NCS ring stretch
1130 m	1129 m	1128 m	1128 m	1127 m	CH in-plane bend
1090 m		1087 w	1076 w	1077 w	Bz ring or SCS antisymmetric stretch
1021 m	1018 m	1009 m	1013 m	1010 m	CH deformation
877 vw	858 m	856 m	855 m	856 m	CH out-of-plane bend
711 w	711 m	711 m	709 m	710 m	CS stretch
617 w	603 w	601 w	601 w	601 w	CS stretch
510 m	502 m	503 m	497 m	501 m	Bz ring deformation
429 m					
406 w	396 m	391 m	393 m	395 m	Bz ring deformation
341 w		344 w			MS stretch

surface. XPS investigations support the conclusion that the surface layer is of monolayer thickness.

Adsorption of the acid form of 2-mercaptobenzothiazole occurs without charge transfer on copper at low potentials at pH 4.6. As the potential is increased, charge transfer occurs and results in the same surface species as in the basic medium.

Acknowledgements

This project was supported by the Australian Research Grants Scheme. The authors are indebted to Cytec Industries Inc. for the supply of the 2-mercaptobenzothiazole. They are also grateful to Dr P.M. Fredericks of the Centre for Instrumental and Development Chemistry for access to Raman instrumentation and to Dr S. Perera for assistance with NMR spectroscopy.

References

1. A.M. Marabini, M. Barbaro and V. Alesse, *Int. J. Miner. Process.* **33** (1991) 291.
2. M. Oshawa and W. Suëtaka, *Corros. Sci.* **19** (1979) 709.
3. A.E. Mantell and R.M. Smith, 'Critical Stability Constants', Vol 3 (Plenum, New York, 1997), p. 313.
4. K. Takahashi, O. Hayashida and Y. Numata, Proceedings of the XVIII International Minerals Processing Congress, Sydney, Aus. IMM (1993), pp. 735–43.
5. N. Sandhyarani, G. Skanth, S. Berchmans, V. Yegnaraman and T. Pradeep, *J. Colloid Interface Sci.* **209** (1999) 154–61.
6. N.P. Finkelstein and G.W. Poling, *Minerals Sci. Eng.* **9** (1977) 177.

7. R. Szargan, I. Uhlig, G. Wittstock and P. Rossbach, *Int. J. Miner. Process.* **51** (1999) 151.
8. A.N. Buckley and R. Woods, *Colloids Surfaces A* **104** (1995) 295.
9. G. Contini, A Ciccioli, C. Cozza, M. Bararo and A.M. Marabini, *Int. J. Miner. Process.* **51** (1997) 283.
10. G.M. Brown, G.A. Hope, D.P. Schweinsberg and P.M. Fredericks, *J. Electroanal. Chem.* **380** (1995) 161.
11. R.C. Bott, G.A. Bowmaker, C.A. Davis, G.A. Hope and B.E. Jones, *Inorg. Chem.* **37** (1998) 651.
12. R. Woods and G.A. Hope, *Colloids Surfaces A* **146** (1999) 63.
13. R. Woods and G.A. Hope, *Colloids Surfaces A* **137** (1998) 319.
14. R. Woods, G.A. Hope and G.M. Brown, *Colloids Surfaces A* **137** (1998) 329.
15. A.N. Buckley, T.J. Parks, A.M. Vassallo and R. Woods, *Int. J. Miner. Process.* **51** (1997) 303.
16. R. Woods, G.A. Hope and G.M. Brown, *Colloids Surfaces A* **137** (1998) 339.
17. I.P. Khullar and U. Agarwala, *Can. J. Chem.* **53** (1975) 1165.
18. M.M. Khan and A.U. Malik, *J. Inorg. Nucl. Chem.* **34** (1972) 1847.
19. M. Fleischmann, D. Sockalingum and M.M. Musiani, *Spectrochim. Acta* **A46** (1990) 285.
20. G.A. Hope, D.P. Schweinsberg and P.M. Fredericks, *Spectrochim. Acta* **A50** (1994) 2019.
21. P.C. Lee, and D. Meisel, *J. Phys. Chem.* **86** (1982) 3391.
22. R. Woods, *in* J.O'M. Bockris, B.E. Conway and R.E. White (Eds), 'Modern Aspects of Electrochemistry', Vol. 29, p. 401.
23. R.-H. Yoon and C.I. Basilio, *in* Proceedings of the XVIII International Minerals Processing Congress, Sydney, Aus. IMM (1993), p. 611.
24. N. Sato and M. Suzuki, *J. Electrochem. Soc.* **135** (1988) 1645.
25. L.A. Goold and N.P. Finkelstein, 'The Reaction of Sulphide Minerals with Thiol Compounds'. Johannesburg, National Institute for Metallurgy, *Report No. 1439*, 29th June (1972), pp. 9.
26. C.L. Brown, private communication (1999).
27. N.B. Colthup, L.H. Daly and S.E. Wiberley, 'Introduction to Infrared and Raman Spectroscopy' (Academic Press, New York, 1975).
28. W.A. Senior and W.K. Thompson, *Nature* **205** (1965) 120.
29. G.E Walrafen, *J. Chem. Phys.* **40** (1964) 3249.
30. A.T. Hubbard, *in* R.G. Compton (Ed), 'Comprehensive Chemical Kinetics', Vol. 28 (Elsevier, Amsterdam, 1989), p. 1.
31. M.M. Walczak, C.A. Alves, B.D. Lamp and M.D. Porter, *J. Electroanal. Chem.* **396** (1995) 103.